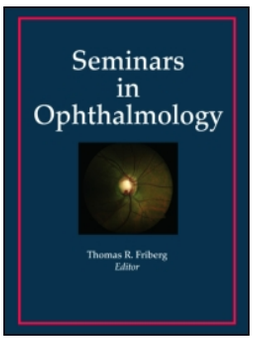

Seminars in Ophthalmology

ISSN: 0882-0538 (Print) 1744-5205 (Online) Journal homepage: https://www.tandfonline.com/loi/isio20

Detection of structural and electrical disturbances in macula and optic nerve in Alzheimer's patients and their correlation with disease severity

Sagnik Sen, Rohit Saxena, Deepti Vibha, Manjari Tripathi, Pradeep Sharma, Swati Phuljhele, Radhika Tandon & Pawan Kumar

To cite this article: Sagnik Sen, Rohit Saxena, Deepti Vibha, Manjari Tripathi, Pradeep Sharma, Swati Phuljhele, Radhika Tandon & Pawan Kumar (2020): Detection of structural and electrical disturbances in macula and optic nerve in Alzheimer's patients and their correlation with disease severity, Seminars in Ophthalmology, DOI: 10.1080/08820538.2020.1748203

To link to this article: https://doi.org/10.1080/08820538.2020.1748203

Published online: 18 Apr 2020.

Seminars in Ophthalmology, Early Online, 1–10, 2020

ISSN: 0882-0538 print / 1744-5205 online
DOI: https://doi.org/10.1080/08820538.2020.1748203

Taylor & Francis
Taylor & Francis Group

ARTICLE

Detection of structural and electrical disturbances in macula and optic nerve in Alzheimer's patients and their correlation with disease severity

Sagnik Sen[1], Rohit Saxena[1], Deepti Vibha[2], Manjari Tripathi[2], Pradeep Sharma[1], Swati Phuljhele[1], Radhika Tandon[1], and Pawan Kumar[1]

[1]*Department of Ophthalmology, AIIMS, New Delhi, India and* [2]*Department of Neurology, AIIMS, New Delhi, India*

ABSTRACT

Aim: To evaluate and compare structural and functional changes in macula and optic nerve in Alzheimer disease (AD) patients and healthy subjects.

Methods: Both eyes of 20 AD patients and 40 age-matched healthy controls were evaluated. All subjects were evaluated by cognitive testing and comprehensive ophthalmological examination, including visual acuity, visual fields, color vision, contrast sensitivity, anterior, and posterior segment examination, optical coherence tomography, multifocal electroretinography (mfERG), and pattern-reversal visual evoked potential (pVEP).

Results: AD patients showed significantly reduced contrast sensitivity, thinner nerve fiber layer, ganglion cell layer andmacular volume. Multifocal ERG wave amplitudes were significantly reduced with delayed implicit times, which correlated significantly with the inner retinal layer thinning and poorer disease severity scores. The correlation with structural changes and disease severity was highest for pVEP, which showed significant derangement in AD patients.

Conclusion: Subclinical visual dysfunction may be present in AD patients, which may be detected as inner retinal thinning. A probable photoreceptor abnormality may also form a part of the AD disease process.

Keywords: Alzheimer's, RNFL, GCL, OCT, mfERG

INTRODUCTION

Alzheimer's disease (AD) is the most common form of dementia in the world with an incidence of 15.54 per 100 person-years (95% CI: 14.6–16.5) in age more than 65 years.[1] The morbidity associated with AD is due to the loss of activities of daily living and a reduced life expectancy. At present, diagnosis of AD is restricted to clinical evaluation with history and neurological examination using cognitive screening and diagnostic tests like National Institute of Neurological and Communication Disorders and Stroke-Alzheimer's disease and Related Disorders association (NINCDS-ADRDA) criteria, Mini-mental state examination scoring (MMSE), Cognitive Dementia Rating (CDR) scale, etc., followed by structural and functional brain imaging.[2] Recent AD research has focused on the detection of downstream neuronal injury that reflects complex patterns of tissue changes through imaging. A number of studies have evaluated spectral-domain optical coherence tomography (OCT) of retina and optic nerve and found characteristic changes in AD patients involving the degeneration of the retinal nerve fiber layer (RNFL) and the retinal ganglion cell layer (RGC).[3–6] Moreover, electrophysiological dysfunction in the retina has been observed in AD using pattern electroretinogram (pERG) and pattern visual evoked potential (pVEP). pVEP and pERG abnormalities may correspond to the affection of RGCs in the inner retinal layers. Another significant question in this regard arises whether the outer retina also gets affected in AD patients. We designed the study in order to evaluate the posterior segment of the eye including the macula and try and find

Received 19 December 2019; accepted 21 March 2020; published online xx xxx xxxx.
Correspondence: Rohit Saxena, Dr Rajendra Prasad Centre for Ophthalmic Sciences, AIIMS, New Delhi, India. E-mail: rohitsaxena80@yahoo.com

a correlation between the structural retinal disease process and the electrical changes in the macula.

METHODS

Study Groups

The study was conducted at a tertiary care center after obtaining approval from the Institutional Ethics Review Board. The study adhered to the tenets of the Declaration of Helsinki and informed consent was taken from all subjects. Each patient needed to have an informant or caregiver. Primary caregivers were considered as surrogate decision-makers and informed consent was obtained from them in case the patient was extremely incapacitated to give consent. A total of 60 subjects (20 AD patients, 40 healthy controls) were included after obtaining written informed consent, the inclusion criteria being age more than 40 years and visual acuity better than 6/9. Sample size was calculated to evaluate a change of 10 μm change of retinal nerve fiber layer thickness from a previous paper evaluating OCT changes in AD.[7] AD patients were diagnosed using the National Institute of Neurological and Communicative Disorders and Stroke and Alzheimer's disease and Related Disorders Association (NINCDS-ADRDA) criteria after consultation with two experienced neurologists. The subjects having other known cerebral pathology, cardiovascular diseases, psychiatric abnormalities, glaucoma/ocular hypertension, macular degeneration, high refractive error of +- 5D and media opacities were excluded. In addition, subjects with head or neck injuries unable to maintain retinal fixation on a specified target were excluded. Disease duration was recorded based on patient and informant's memory of onset of symptoms. Controls comprised of cognitively normal elderly subjects (screened via MMSE score in the Neurology department), age matched within ± 2 years of the AD cases, taken from the outpatient department, without any ophthalmic diseases, neurodegenerative diseases, or cardiovascular risk factors.

Cognitive Scoring

Initial screening using the MMSE score was performed for all subjects (cases and controls) by two Neurologists. Detailed evaluation of cognition of the AD cases using Global Deterioration Scale and Washington University Clinical Dementia Rating (CDR) scale was performed by two neurologists.[8,9] The patients were rated in each domain according to their cognitive functionality and the final score was determined based on an algorithm of clinical scoring rules after incorporating information from both the patient and the informant. The sum of boxes score of CDR (CDR-SOB) was also calculated for each patient.

Ophthalmic Evaluation

All subjects underwent comprehensive ophthalmological evaluation for each eye separately including best-corrected visual acuity (BCVA) measured using ETDRS charts, colour vision using Ishihara pseudoisochromatic test plates, contrast sensitivity using Pelli-Robson chart and anterior and posterior segment examination. The subjects were required to take adequate sleep the night before ocular investigations to ensure compliance. All subjects were evaluated using a spectral-domain optical coherence tomography (OCT) device (Cirrus HD-OCT Model 4000, Carl Zeiss Meditec Inc., Dublin, CA). Analyzed features included retinal nerve fiber layer (RNFL) thickness in the 200 × 200 scan and ganglion cell layer (GCL) thickness and macular volume (MV) in the 512 × 128 scan. All scans deemed suitable for gradation in the study had a signal strength of at least 5 and re-scanning was performed if any motion artefact was detected. MfERG was performed according to ISCEV standards using a 61-scaled hexagon display (Metrovision, Monpack, Pirenchies, France) with a mean luminance of 100 cd/m2 and a contrast of >90%.[10] Disposable monopolar scleral lenses and skin electrodes were used for mfERG. The display monitor was placed at a distance of 30 cm before the patient and one eye was tested at a time. Stimulus frequency of the hexagon display was kept at 17 Hz. Video monitoring based on a near infra-red sensor which recorded image of the eye was used for ensuring and monitoring eye-fixation. Five thousand responses were recorded over a period of 5 min for each eye. First-order kernel mfERG responses were documented for further analysis. Pattern-reversal VEP was also performed according to ISCEV standards using a single recording channel with a midline occipital positive electrode.[11] This active skin electrode was placed at the Oz position, the highest point of the occiput, with reference and ground electrodes at Fz and Cz (vertex) points, respectively. Recording was performed using the Nicolet Ganzfeld 2015 visual stimulator and a monitor (Nicolet Biomedical, Madison, WI). A checkerboard pattern (reversal time of 500 ms) was used with a field size of >150 and mean luminance of 50 cd/m2, kept at a distance of 100 cm from the subjects' eye. The monitor presented black and white checks, whose phases were reversed, i.e., black to white and white to black, at a fixed rate of two reversal per second. Each eye was tested separately. A sweep length of 250 ms was used which recorded

more than 100 responses, at an amplification range of 20000 to 100000. Electrode impedance was kept less than 5 KΩ. Visual fields were recorded using automated Visual Field Analyser 750i (Carl Zeiss Meditec, Dublin, CA) with 30–2 SITA Standard Strategy. Automated static field results were considered reliable if false-positive and false-negative responses were lower than 33% and fixation loss lesser than 20%. MfERG, pattern VEP and fields were tested with the patient wearing full refractive correction.

All investigations were done by one Neuro ophthalmology laboratory personnel. The patient's name and identification number only were revealed to the person and whether the subject was a part of any study or that he suffered from a particular disease condition was not revealed to him.

Statistical Analysis

Data were analysed using IBM SPSS Statistics version 21.0 (Armonk, NY). Generalized estimating equations (GEE) adjusted for age and inter-eye correlation were used to compare variables between AD patients and controls. In the GEE model, age was taken as a between-subject effect and eye of the patient as a within-subject effect. Disease status (Alzheimer's or healthy control) was kept as a dependent variable. Binary logistic model was used for GEE. The robust estimator matrix was used with an independent working correlation matrix to adjust estimators by number of non-redundant parameters. Eye (right or left) was considered a factor and age a covariate in the analysis. Pearson's correlation coefficients were used to correlate variables and determine the strength of such correlations. Receiver operating characteristic (ROC) curves were obtained to describe the discrimination ability of parametres by the area under the curves (AUC). Data was considered statistically significant for a 2-tailed p value of 0.05. For multiple comparisons within a given domain, to compare several parameters, modified p values using Bonferroni correction were used.

RESULTS

Demographics

The study evaluated 120 eyes of 20 cases of clinically diagnosed AD patients and 40 cognitively healthy control subjects (Table 1). Table 1 displays the GEE parameter estimates (p values and 95% confidence intervals) and the AUC obtained by the ROC curves. The mean (SD) age of AD patients was 61.5 (7.45) years (range, 45–78 years), that of controls being 60.94 (7.6) years (range, 44–72 years) (p = .79).

The median MMSE score was 17.5 (range, 10–23) in AD patients and 28 (range, 26–29) in controls (Table 2). The median severity of disease (CDR) was 1 (range, 0.5–2) and the median sum-of-boxes CDR score was 5.5, indicating a mild dementia. The median duration of disease was 2 years (range, 6 months-3.5 years). The mean (SD) BCVA was similar in the two groups (p = .19). Mean contrast sensitivity was significantly reduced in the AD eyes (p < .05) (Table 1). Static visual fields were found to be within normal limits in all patients. The anterior segment, intraocular pressure, fundus examination, and colour vision were within normal limits in all subjects.

OCT Measurements

AD patients showed significant average RNFL thinning with individual significant thinning (Table 1) in superior and inferior quadrants of RNFL (p < .001) with the largest AUCs being for superior (0.863; 95% CI: 0.791–0.937) and inferior (0.8; 95% CI: 0.718–0.888) quadrants. The ratio of nasal to temporal RNFL thickness was higher in AD eyes (p < .001) indicating thinner papillomacular bundle. AD eyes showed significant average GCL thickness reduction compared to controls; individually in superior, superonasal, inferonasal, inferior, inferotemporal, and superotemporal sectors (p < .005) (Table 1). The inferotemporal quadrant showed the largest AUC (0.887; 95% CI: 0.826–0.948), followed by the superior quadrant (0.883; 95% CI: 0.812–0.955). AUC of RGCL average (0.947; 95% CI: 0.909–0.985) was higher than that of RNFL average (0.892; 95% CI: 0.832–0.953). Also, macular volume thinning was observed in the AD patients (p < .001).

Electrophysiological Parameters

A generalized suppression of electrical activity was observed in mfERG (Table 1). The mfERG anatomical areas corresponded to the following: ring 1 to fovea, ring 2 to parafovea, ring 3 to perifovea, ring 4 to near periphery, and ring 5 to mid-periphery. Mean P1, N1, and N2 amplitudes were significantly reduced (p < .001) in AD cases in rings 1–5, while mean P1 implicit times were significantly prolonged (p < .001) in rings 1–5. N1 and N2 implicit times were longer in AD group than healthy controls, however, the difference was not found significant. Pattern –reversal VEP amplitude was significantly reduced with latency prolonged significantly in the AD patients (p < .05). VEP latency was higher than 115 ms in 26/40 eyes (65%). Ten AD patients (50%) had bilateral prolongation (20 eyes) of VEP latency while the rest six patients showed this unilaterally. Analysis of AUC

TABLE 1. Comparative evaluation of Alzheimer's patients and healthy controls.

	Cases (N = 40)	Controls (N = 80)	Difference (95% CI)[c]	S.E.	p value[a]	Effect size[d]	AUC (95% CI)[b]
Age	61.5 ± 7.45 (N = 20)	60.94 ± 7.6 (N = 40)			0.79		
BCVA (logMAR)	0.17 ± 0.132 (N = 40)	0.14 ± 0.112 (N = 80)			0.19		
Contrast sensitivity	1.326 ± 0.205 (N = 40)	1.853 ± 0.05 (N = 80)	−0.53 (−0.58, −0.47)	0.02	***<0.05***	4.22	
Retinal nerve fibre layer thickness (µm)							
Superior quadrant	76.2 ± 28.56	112.34 ± 15.87	−33.8 (−47.9, −19.7)	7.21	***<0.001***	1.72	0.863 (0.791–0.937
Nasal quadrant	62.83 ± 16.69	71.23 ± 10.19	−4.4 (−10.3, 1.5)	3.0	0.141	0.66	0.683 (0.566–0.8)
Inferior quadrant	77.08 ± 25.09	105.88 ± 23.29	−23.1 (−36.4, −9.7)	6.82	***<0.001***	1.21	0.803 (0.718–0.888)
Temporal	53.23 ± 19.09	60.5 ± 11.83	−7.6 (−15.3, −0.4)	3.89	0.049	0.497	0.653 (0.544–0.761)
Average	67.33 ± 13.14	87.49 ± 9.2	−17.2 (−24.0, −10.5)	3.45	***<0.001***	1.89	0.892(0.832–0.953)
Retinal ganglion cell layer thickness (µm)							
Superior sector	68.38 ± 19.59	90.41 ± 8.6	−21.8 (−28.3, −15.3)	3.32	***<0.001***	1.66	0.883 (0.812–0.955)
Supero-nasal sector	67.93 ± 17.83	85.95 ± 8.83	−18.6 (−24.1, −13.1)	2.79	***<0.001***	1.44	0.871 (0.805–0.936)
Infero-nasal sector	66.75 ± 17.17	85.24 ± 8.29	−15.9 (−21.8, −9.9)	3.02	***<0.001***	1.54	0.861 (0.796–0.927)
Inferior sector	58.78 ± 18.78	81.44 ± 13.79	−18.2 (−26.4, −10.1)	4.15	***<0.001***	1.78	0.859 (0.788–0.93)
Inferotemporal	61.93 ± 18.19	85.23 ± 7.72	−24.3 (−31.9, −16.7)	3.89	***<0.001***	1.9	0.887 (0.826–0.948)
Supero-temporal sector	65.2 ± 18.86	87.46 ± 9.64	−20.6 (−27.3, −13.9)	3.43	***<0.001***	1.66	0.883 (0.818–0.947)
Average	64.83 ± 13.74	85.95 ± 6.28	−19.9 (−24.8, −14.9)	2.51	***<0.001***	2.24	0.947 (0.909–0.985)
Macular volume (mm^3)	8.92 ± 0.78	9.78 ± 0.64	−0.83 (−1.15, −0.52)	0.15	***<0.001***	1.25	0.872 (0.801–0.944)
mfERG Amplitudes (nV)							
P1 wave							
Ring 1	990.38 ± 406.34	1495.58 ± 378.56	−448.3 (−656.1, −240.5)	106.0	***<0.001***	1.3	0.859 (0.775–0.943)
Ring 2	720.38 ± 235.25	1116.3 ± 263.87	−320.3 (−4393, −201.3)	60.71	***<0.001***	1.55	0.859 (0.789–0.93)
Ring 3	794.05 ± 296.4	1049.75 ± 223.87	−200.4 (−305.9, −94.8)	53.8	***<0.001***	1.02	0.816 (0.734–0.898)
Ring 4	804.6 ± 233.65	1080.78 ± 231.84	−226.3 (−341.08, −111.5)	58.57	***<0.001***	1.19	0.788 (0.698–0.878)
Ring 5	958.73 ± 296.4	1160.3 ± 255.39	−168.9 (−297.6, −40.2)	65.65	0.01	0.747	0.698 (0.594–0.801)
Average	853.62 ± 228.93	1180.54 ± 237.65	−272.8 (−390.1, −155.5)	59.84	***<0.001***	1.39	0.836 (0.757–0.915)
N1 wave							
Ring 1	497.85 ± 211.254	876.45 ± 187.94	−360.7 (−462.7, −258.7)	52.06	***<0.001***	1.93	0.921 (0.859–0.984)
Ring 2	445.73 ± 209.27	599.77 ± 162.49	−114.2 (−192.3, −36.1)	39.8	***<0.001***	0.859	0.769 (0.658–0.878)
Ring 3	421.13 ± 133.39	539.33 ± 126.93	−105.4 (−171.3, −39.6)	33.6	***<0.001***	0.91	0.775 (0.674–0.877)
Ring 4	403.08 ± 97.79	515.19 ± 105.55	−100.5 (−148.1, −52.8)	24.31	***<0.001***	1.09	0.799 (0.703–0.892)
Ring 5	488.13 ± 188.94	538.1 ± 118.63	−46.1 (−122.3, 30.1)	38.8	0.236	0.34	0.709 (0.601–0.817)
Average	451.18 ± 122.12	613.77 ± 104.32	−145.4 (−199.1, −91.6)	27.43	***<0.001***	1.47	0.843 (0.75–093)
N2 wave							
Ring 1	751.35 ± 314.75	1399.65 ± 435.44	−776.7 (−1015.8,-537.6)	122.0	***<0.001***	1.62	0.901 (0.835–0.966)
Ring 2	639.08 ± 213.71	927.99 ± 192.47	−300.8 (−406.7, −195.0)	53.9	***<0.001***	1.45	0.85 (0.768–0.932)
Ring 3	581.96 ± 215.11	864.17 ± 205.15	−311.8 (−422.1, −201.6)	56.23	***<0.001***	1.35	0.838 (0.755–0.92)
Ring 4	672.65 ± 181.28	807.62 ± 286.05	−125.6 (−239.8, −11.28)	58.27	0.031	0.53	0.723 (0.627–0.819)
Ring 5	789.33 ± 285.99	942.99 ± 258.93	−194.9 (−316.16, −73.8)	61.8	***<0.001***	0.57	0.638(0.528–0.749)
Average	686.87 ± 189.43	988.48 ± 199.42	−341.9 (−442.9, −240.9)	51.53	***<0.001***	1.54	0.849 (0.77–0.928)
P100 wave							
Amplitude (µV)	7.62 ± 2.97	11.04 ± 2.89	−3.3 (−4.7, −1.8)	0.75	***<0.05***	1.17	0.825 (0.742–0.908)
mfERG Implicit times (ms)							
P1 wave							
Ring 1	51.36 ± 3.73	47.13 ± 4.47	3.9 (2.1, 58)	0.93	***<0.001***	0.997	0.781 (0.699–0.864)
Ring 2	49.31 ± 4.8	45.13 ± 3.29	3.7 (2.2, 5.2)	0.75	***<0.001***	1.08	0.827 (0.746–0.909)

Ring 3	48.2 ± 5.35	44.03 ± 3.48	4.07 (2.4, 5.7)	0.84	***<0.001***	0.994	0.785 (0.694–0.876
Ring 4	48.61 ± 5.44	43.72 ± 3.29	4.25 (2.6, 5.9)	0.84	***<0.001***	1.185	0.81 (0.73–0.889)
Ring 5	48.42 ± 5.36	43.26 ± 3.29	4.3 (2.7, 6.04)	0.85	***<0.001***	1.26	0.818 (0.736–0.9)
Average	49.18 ± 4.47	44.65 ± 3.3	4.07 (2.58, 5.57)	0.76	***<0.001***	1.21	0.837 (0.762–0.911)
N1 wave							
Ring 1	31.1 ± 6.46	26.27 ± 3.59	3.9 (1.7, 6.2)	1.1	***<0.001***	1.02	0.813 (0.73–0.894)
Ring 2	28.42 ± 5.55	26.62 ± 3.92	2.04 (−0.5, 4.1)	1.1	0.056	0.39	0.678 (0.566–0.792)
Ring 3	28.31 ± 4.84	26.23 ± 3.5	2.3 (0.58, 4.1)	0.9	0.009	0.52	0.74 (0.64–0.839)
Ring 4	28.6 ± 5.29	26.3 ± 3.4	2.2 (0.46, 4.0)	0.9	0.014	0.56	0.724 (0.629–0.82)
Ring 5	27.9 ± 6.67	25.9 ± 4.93	2.8 (−0.11, 5.7)	1.48	0.059	0.36	0.645 (0.536–0.753)
Average	28.87 ± 5.19	26.27 ± 3.4	2.67 (0.78, 4.6	0.97	0.006	0.64	0.746 (0.65–0.843)
N2 wave							
Ring 1	71.03 ± 5.49	67.38 ± 6.9	3.9 (0.87, 7.1)	1.58	0.012	0.56	0.739 (0.646–0.831)
Ring 2	66.12 ± 4.67	64.18 ± 6.14	1.3 (−1.07, 3.7)	1.21	0.281	0.34	0.685 (0.587–0.784)
Ring 3	62.23 ± 9.69	62.42 ± 5.77	1.57, (−0.74, 3.9)	1.18	0.183	0.02	0.645 (0.543–0.747)
Ring 4	63.79 ± 4.69	61.9 ± 5.65	1.21 (−1.17, 3.6)	1.21	0.32	0.35	0.701 (0.605–0.97)
Ring 5	63.22 ± 4.07	61.58 ± 5.45	1.62 (−0.59, 3.8)	1.12	0.15	0.32	0.685 (0.585–0.784)
Average	65.28 ± 4.32	63.49 ± 5.65	1.93 (−0.37, 4.2)	1.18	0.1	0.34	0.725 (0.63–0.819)
P1/N1							
Ring 1	1.76 ± 0.5	2.11 ± 0.66	0.34 (0.03, 0.65)	0.16	0.029	0.57	0.318 (0.215–0.944)
Ring 2	1.85 ± 0.73	1.95 ± 0.61	−0.106 (−0.47, 0.26)	0.19	0.568	0.15	0.526 (0.411–0.642)
Ring 3	2.01 ± 0.64	2.03 ± 0.58	0.07 (−0.26, 0.39)	0.17	0.692	0.03	0.521 (0.411–0.632)
Ring 4	2.06 ± 0.59	2.16 ± 0.58	−0.06 (−0.35, 0.23)	0.15	0.673	0.17	0.525 (0.413–0.638)
Ring 5	2.09 ± 0.66	2.23 ± 0.61	−0.103 (−0.39, 0.19)	0.15	0.484	0.22	0.552 (0.437–0.668)
Average	2.03 ± 0.49	2.02 ± 0.47	0.027 (−0.24, 0.04)	0.13	0.838	0.02	0.489 (0.379–0.599)
P100 wave							
Latency (ms)	120.01 ± 6.99	108.36 ± 4.84	12.0 (8.8, 15.1)	1.61	***<0.05***	2.06	0.94 (0.897–0.982)

[a]Generalised estimating equations paramter estimates.
[b]Area under Receiver operator characteristic curve.
[c]Wald's 95% confidence intervals as determined in GEE model.
[d] Effect size calculated by Hedge's g.
S.E.: Standard error
BCVA: Best-corrected visual acuity.
logMAR: log of minimum angle of resolution.
mfERG: multifocal electroretinogram.
CI: Confidence interval.
Bold signifies significant p values after considering multiple comparisons (Bonferroni)
AUC: area under curve.

TABLE 2. Disease characteristics of AD cases (Median).

AD cases (N = 20)	
Disease duration (years)	2
Mini Mental State Examination score	17.5
Global Deterioration Scale score	4
Global Cognitive Dementia Rating score	1
Cognitive Dementia Rating Scale Sum-of-boxes score	5.5

of the ROC curves (Table 1) of mfERG and pattern VEP revealed largest AUC of P100 latency (AUC = 0.94; 95% CI: 0.897-.982) followed by N1 ring 1 amplitude (AUC = 0.921; 95% CI: 0.859–0.984), N2 ring 1 amplitude (AUC = 0.901; 95% CI: 0.835–-0.966) and P1 ring 1 amplitude (AUC = 0.859; 95% CI: 0.775–0.943).

Correlation of Structural and Functional Parameters with Disease Characteristics

Disease duration significantly correlated with contrast sensitivity reduction (r = −0.34, p = .042) (Table 3). Contrast sensitivity reduction was positively correlated with P100 amplitude (r = 0.385, p = .014). No correlation was found among MMSE scores and OCT or electrophysiological parametres. However, disease severity denoted by CDR-SOB was found to have negative correlation with RNFL average thickness (r = −0.596, p < .001) and also independently with RNFL thickness superior quadrant (r = −0.476, p = 0,002) and inferior quadrant (r = −0.383, p = .015). CDR-SOB also correlated with P1 average amplitude (r = −0.41, p = .009) and P100 amplitude (r = −0.333, p = .036). RNFL average thickness had positive association with RNFL thickness in superior quadrant (r = 0.771, p < .001) and RGCL thickness in superior sector (r = 0.388, p = .013) and infero-nasal sector (r = 0.322, p = .043).

TABLE 3. Summary of correlation among disease duration, MMSE, and CDR scale with the structural and functional changes detected in eyes of AD cases (N = 40) ([a]Pearson's correlation coefficient).

		r[a]	*P value*
Duration	Contrast	−0.34	***.042***
	RGCL supero-nasal sector	−0.367	***.028***
	RGCL average	−0.34	***.042***
	P1 amplitude average	−0.447	***.006***
	P1/N1 average	−0.414	***.012***
MMSE	P1/N1 average	−0.572	***<.001***
CDR sum of boxes	RNFL superior quadrant	−0.476	***.002***
	RNFL inferior quadrant	−0.383	***.015***
	RNFL average	−0.596	***<.001***
	P1 amplitude average	−0.41	***.009***
	P100 amplitude	−0.333	***.036***

MfERG and pattern VEP amplitudes were positively correlated with RNFL average thickness and negatively correlated with P100 latency (r = −0.4, p = .011) (Table 4). GCL average thickness was correlated independently with GCL infero-nasal sector (r = 0.853, p < .001) followed by inferior sector thickness (r = 0.828, p < .001) and with P100 amplitude (r = 0.331, p = .037). Macular volume was positively correlated with GCL thickness in infero-temporal sector (r = 0.331, p = .037). P100 amplitude positively correlated with mfERG amplitudes.

Agreement between Cognitive Scales Used (Table 5)

Subgroup analysis was done to compare the discriminant abilities of the two scoring systems used to categorize patients into different stages of AD. It was observed that six patients labelled as mild AD by CDR were staged as moderate AD by GDS. Only two eyes were staged as belonging to a severe AD case, hence they were not included for analysis. The

TABLE 4. Correlation between structural and functional changes detected in inner and outer layers of retina in AD eyes (N = 40) ([a]Pearson's correlation coefficient).

		r[a]	*P value*
Contrast sensitivity	p100 amplitude	0.385	***.014***
RNFL average	RNFL superior quadrant	0.771	***<.001***
	RNFL inferior	0.682	***<.001***
	RNFL temporal	0.458	***.003***
	RGCL superior sector	0.388	***.013***
	RGCL infero-nasal	0.322	***.043***
	P1 amplitude average	0.454	***.003***
	N1 amplitude average	0.417	***.007***
	N2 amplitude average	0.408	***.009***
	P100 amplitude	0.698	***<.001***
	P100 latency	−0.4	***.011***
RGCL average	RGCL superior sector	0.779	***<.001***
	RGCL supero-nasal	0.825	***<.001***
	RGCL infero-nasal	0.853	***<.001***
	RGCL inferior	0.828	***<.001***
	RGCL infero-temporal	0.575	***<.001***
	RGCL supero-temporal	0.621	***<.001***
	P100 amplitude	0.331	***.037***
Macular volume	RGCL inferotemporal	0.331	***.037***
P100 amplitude	RNFL average	0.698	***<.001***
	RGCL average	0.331	***.037***
	RMS average	0.505	***.001***
	P1 amplitude average	0.463	***.003***
	N1 amplitude average	0.495	***.001***
	N2 amplitude average	0.365	***.02***
	N2 time average	−0.577	***<.001***
	P100 latency	−0.355	***.025***
P100 latency	RNFL superior	−0.323	***.042***
	RGCL supero-nasal	−0.314	***.049***
	RNFL average	−0.4	***.011***
	P1 amplitude	−0.349	***.027***
	P100 amplitude	−0.355	***.025***

TABLE 5. Comparison of AD cases scored according to the two scales used.

		CDR		
		Mild	**Moderate**	Total
GDS	**Mild**	13	0	13
	Moderate	3	3	6
	Total	26	3	19

two scoring systems were found to have a moderate agreement (Cohen's kappa = 0.5778, 95% CI: 0.18 - 0.975) with each other.

DISCUSSION

AD patients in our study demonstrated normal visual acuity in the presence of significantly reduced contrast sensitivity. Our study patients were comparatively in the milder stages of dementia explaining differing results in comparison to other reports, which have reported reduced visual acuity.[12] The median scores of CDR and GDS scales both indicated the presence of mild dementia with moderate concordance between the two scales used. Although frank visual deficit may occur only in the advanced stages of the disease, almost 43% of early AD patients may have complex visual symptoms like defects in contrast sensitivity, right left distinction, visuomotor skill impairment, prosopagnosia, hallucinations, complex deficits in colour vision, Balint's syndrome, etc.[13] This visual dysfunction was earlier thought to be due to aberrations in the visual cortex and higher cortical areas; however, pre-cortical degeneration has also been suggested to be playing a role.[2,3,6]

Obtaining the ophthalmological tests was a quite challenging task for the laboratory personnel since AD patients were often uncooperative and needed to be in a lucid state to clearly understand and follow commands. Hence, the caregivers were asked to ensure that all subjects were well rested after a good night's sleep before performing the ophthalmological investigations. All subjects were initially made comfortable in the presence of the primary caregiver before performing the tests, and then only testing was started, with adequate importance given to the maintenance of fixation. The electrophysiology station had a fixation monitor on screen which was used to ascertain maintenance of fixation throughout the duration of the tests.

Structural Changes

We found that RNFL and RGCL thickness were significantly reduced in all quadrants. A number of studies has shown RNFL thinning using both time-domain and spectral-domain OCT machines with similar findings.[2,3,13] RNFL thinning has been hypothesized to be due to a degeneration of the GCL axons which may precede the cognitive impairment in AD.[14,15] Advanced OCT technology allowed us to analyze the GCL separately from RNFL and nullified the effect of variability of RNFL in healthy population, in contrast to previous literature where the two layers have been studied together. Till date, few studies have separately analyzed GCL on OCT and found significantly reduced overall GCL thickness in AD eyes.[16,17]

Interestingly, most studies have shown a significant reduction of RNFL thickness in all quadrants of retina, but more predominantly in the superior and inferior quadrants.[18,19] In our study, higher AUCs for RNFL thickness reduction were seen in the superior and inferior quadrants and AUC of GCL was maximum in the inferotemporal and superior sectors, thereby corresponding to the changes in RNFL. Our observations may have reflected the fact that maximum number of nerve fibers converge on the optic disc superiorly and inferiorly and hence, neurodegeneration affected them preferentially. These changes were further reflected in the significant loss of macular volume in the AD group. In addition, based on the AUC findings, we infer that GCL may be a better indicator of disease status than RNFL, which is similar to one previous OCT-based study.[16] GCL thinning may precede loss of neurons in hippocampus of human brain, similar to what has been seen in mouse models of AD.[20] However, all of our AD patients already demonstrated cortical atrophy when we evaluated them, probably because of which the global GCL thinning was noted.

Functional Changes

In mfERG, we found significant reduction of P1, N1, and N2 amplitudes with a significantly higher P1 implicit time in the foveal (central 2°) and parafoveal (2–15°) regions. One study has reported similar results previously.[21] Detection of mfERG dysfunction in AD cases was peculiar, and although the exact cause cannot be pointed out, it may be due to an underlying outer retinal involvement, probably secondary to local amyloid deposition.[22] This needs to be investigated further with pattern ERG and targeted investigations for the detection of local amyloid in the retina and by correlating them with structural parameters.

We found a reduced amplitude and prolonged latency of pattern VEP in AD cases. AD patients have previously been reported to have an abnormal flash VEP with prolonged latency of the positive component.[23] But pattern VEP studies have been equivocal, with varying results.[24,25] This change in pattern VEP may be because of an underlying

macular dysfunction, as has been proposed previously.[26] pVEP measures the integrity of the entire visual pathway. Since all of our AD patients had presence of cortical atrophy, this may also be the reason for deranged VEPs. We found that AUC of P100 latency was highest among all the electrophysiological parameters indicating that pattern reversal VEP may be a better predictor of the electrical disturbance in AD. We did not detect any changes in the visual fields of the patients and the threshold readings were within normal limits.

Correlation between Structural and Functional Changes

Significant correlation found between contrast sensitivity reduction and pattern VEP amplitude signifies the early subclinical electrical disturbance in the neural system in AD. Disease duration also correlated with severity of OCT and mfERG changes in AD patients with patients having longer duration having more severe affection of the macula. While trying to correlate the disease severity scores with the ophthalmological investigations, we could find no correlation of MMSE with the investigations. Disease severity measured as CDR-SOB correlated significantly with OCT and electrophysiological derangement, the strongest correlation being with average RNFL thickness. This again reemphasizes the role of OCT in identifying retinal thinning and indicating a simultaneous analogy to the severity of the AD disease process also, which is a novel finding of our study.

We found that structural alterations in inner retinal layers on OCT were correlated significantly with foveal electrical dysfunction detected by mfERG. This structural-functional correlation was manifested only as a subclinical contrast sensitivity impairment since the visual acuities were normal for all subjects. OCT changes also correlated with pattern VEP amplitude and average RNFL thickness. Previously, AD patients have been shown to have a significant correlation between the VEP latency and disease severity and VEP amplitude with disease duration.[26] Since we did not perform detailed cognitive and psychophysical status evaluation of patients, we were not able to establish the extent of neurological defects present in the patients, e.g., apraxia or aphasias affecting the ocular function.

Concept of Retinal Amyloid

Our findings may shed some light on the involvement of retina in AD. Recently ocular AD has been described, which involves localized amyloid deposition in the retina. Previously, histological studies in retina from AD patients have found a vacuolated and 'frothy' appearance of the cytoplasm of degenerated RGCs instead of characteristic neurofibrillary tangles which is rather unique to AD.[27] Koronyo-Hamaoui et al. first visualized curcumin bound fluorescent amyloid beta (Aβ) in the retinas of transgenic mice.[28] Such curcumin binding of Aβ has also been demonstrated in the retina and brain of AD donors, although this was absent in healthy controls. Although, Aβ accumulation in photoreceptor outer segments associated with electrophysiological abnormalities has been seen in few animal models, photoreceptor death has not been noted in the progressed stages in another mouse AD model.[29,30] Few studies have reported Aβ plaques in the GCL with ganglion cell destruction along with electrophysiological dysfunction.[31,32] Recent mice studies also have shown an association between retinal Aβ burden and inner retinal function.[33,34] It is of importance that the GCL cell body destruction has been seen to precede the loss of dendrites in hippocampal pyramidal neurons in Tg2576 mice with frank pathological changes of AD.[20] Non-invasive hyperspectral imaging technology of retina also suggests that early Aβ deposition-related retinal dysfunction may begin during the asymptomatic stage of AD.[35] In contrast to these findings, absence of Aβ deposits in retina of confirmed AD patients has also been reported.[36] Recently, demonstration of tau deposits in the retina of 301 S human tau mouse line using in vivo scanning laser ophthalmoscopy, and also in AD patient retina, has led authors to suggest that hyperphosphorylated tau proteins in retina may also be another marker for AD.[37] Neuroscientists are unclear as to whether Aβ accumulation facilitates the pathogenicity of tau in the cortex or tau accumulation precedes diffuse cortical Aβ deposition.[36] To what extent this amyloid is pathogenetic in the retina or whether it is just an age-related change is unknown. Moreover, whether ocular AD is a completely different disease process or a part of the same spectrum as AD is also not known for sure. However, our findings may indicate the possibility of a primary photoreceptor dysfunction in AD patients apart from the ganglion cell dysfunction. A pattern ERG-based evaluation may be more specific towards the same.

Future Direction

The primary diagnosis of Alzheimer's disease is based on NINDS-ADRDA clinical criteria and on a battery of cognitive tests like the MMSE, CDR, etc., supplanted by imaging modalities like MRI and FDG-PET. Efforts have been on for the identification of biomarkers for preclinical diagnosis of Alzheimer's or screening of patients at risk of Alzheimer's before definite cerebral atrophy sets in. The next generation of imaging for AD

diagnosis is targeted towards detection of amyloid/tau in brain and retina before the onset of full-fledged dementia, based on the observation that retinal Aβ deposits precede brain Aβ deposition.[38] PET imaging targeted for tau or Aβ deposition early in the disease, in the inferior temporal cortex has been considered an early AD biomarker; however, the invasiveness of this test is a drawback. In this regard, as a non-invasive rapid screening or diagnostic tool, ocular examination is believed to gain an important status in future. Ganglion cell layer, contrast sensitivity, and mfERG have the potential to become sensitive indicators in early disease stages, with a significant correlation with disease attributes. Reduction of total brain volume has been found to have a weak association with GCL thinning; however, reduction of grey matter volume in occipital and temporal lobes has been seen to be strongly associated with GCL thinning, independent of systemic vascular risk factors.

Although OCT can assess this small part of the CNS (viz. retinal layers) with high accuracy, as seen in our findings, however, it has to be determined if these patterns are exclusive to AD. Recently, deep-learning-based tools of artificial intelligence (AI) have been studied to understand the progression and referral patterns of retinal diseases using OCT.[39] Also, a recurrent neural network-based predictive model for AD progression has been developed using the GDS and CDR scales.[40] However, they have not included more accurate diagnostic testing for AD, e.g., AD biomarkers. In future, such AI models may be developed, incorporating OCT and electrophysiology data along with cognitive classification schemes to accurately predict the progression from cognitively normal to dementia stage.

The limitation of this study was that we did not evaluate mild cognitive impairment cases and hence could not record the natural history of structural and electrophysiological changes, because of design limitations. Pattern electroretinogram is a more useful test for targetedly ascertaining ganglion cell dysfunction and this may be analysed in AD patients in a future study. We also lacked in the number of patients with severe AD who could cooperate for the study. The repeatability and consistency of the tests need to be ascertained by conducting large-scale population-based studies to minimise chances of false positives. Moreover, we did not use any targeted investigation to detect pathology in the photoreceptor layer of the macula which may have given rise to the electrical changes that we detected. Few studies believe that these changes are because of local Aβ deposition, but whether this is a part of the overall AD pathogenesis is not clear. Larger studies utilising markers for such deposits and correlating their presence with cognitive status of patients may give us some answers.

Conclusion

Detection of inner retinal thinning, especially GCL thinning, along with pre-determined cut-offs by OCT may help improve the diagnostic accuracy of AD in the earliest stages, as observed by the correlation between these parameters and electrophysiological disturbances and disease severity, whereas neuroimaging modalities can only pick up changes in the central nervous system with established atrophy.

AUTHORSHIP STATEMENT

Authors' contributions: SS, RS, MT, DV, PS, RT, SP were involved in study design. SS, RS, MT, and DV were involved in data collection. SS and RS performed the data analyses. RS, MT, and DV provided guidance about the data analysis, interpretation, and presentation of the data. PK helped in ophthalmic investigations. All authors critically reviewed and edited the article. The authors have no funding sources to declare.

ORCID

Sagnik Sen http://orcid.org/0000-0001-5835-5371

DATA AVAILABILITY

With authors, will be made available on request.

REFERENCES

1. Mathuranath PS, George A, Ranjith N, et al. Incidence of Alzheimer's disease in India: a 10 years follow-up study. *Neurol India*. 2012;60:625–630. doi:10.4103/0028-3886.105198.
2. Blacker D, Albert MS, Bassett SS, et al. Reliability and validity of NINCDS-ADRDA criteria for Alzheimer's disease. The National Health Institute of Mental Health Genetics initiative. *Arch Neurol*. 1994;51:1198–1204. doi:10.1001/archneur.1994.00540240042014.
3. Iseri PK, Altinaş O, Tokay T, Yüksel N. Relationship between cognitive impairment and retinal morphological and visual functional abnormalities in Alzheimer disease. *J Neuroophthalmol*. 2006;26:18–24. doi:10.1097/01.wno.0000204645.56873.26.
4. Güneş A, Demirci S, Tök L, Tök Ö, Demirci S. Evaluation of retinal nerve fiber layer thickness in Alzheimer's disease using spectral-domain optical coherence tomography. *Turk J Med Sci*. 2014;44:1–4.
5. Guo L, Duggan J, Cordeiro MF. Alzheimer's disease and Retinal Neurodegeneration. *Curr Alzheimer Res*. 2010;7:3–14. doi:10.2174/156720510790274491.
6. Berisha F, Feke GT, Trempe CL, et al. Retinal abnormalities in early Alzheimer's disease. *Invest Ophthalmol Vis Sci*. 2007;48:2285–2289. doi:10.1167/iovs.06-1029.

7. Marziani E, Pomati S, Ramolfo P, et al. Evaluation of retinal nerve fiber layer and ganglion cell layer thickness in Alzheimer's disease using spectral domain optical coherence tomography. *Invest Ophthalmol Vis Sci*. 2013;54:5953–5958. doi:10.1167/iovs.13-12046.
8. Reisberg B, Ferris SH, de Leon MJ, Crook T. The global deterioration scale for assessment of primary degenerative dementia. *Am J Psychiatry*. 1982;139:1136–1139.
9. O'Bryant SE, Waring SC, Cullum CM, et al. Staging dementia using clinical dementia rating scale sum of boxes scores: a Texas Alzheimer's research consortium study. *Arch Neurol*. 2008;65:1091–1095. doi:10.1001/archneur.65.8.1091.
10. Hood DC, Bach M, Brigell M, et al. ISCEV standard for clinical multifocal electroretinography (mfERG) (2011 edition). *Doc Ophthalmol*. 2012;124:1–13. doi:10.1007/s10633-011-9296-8.
11. Odom JV, Bach M, Brigell M, et al. ISCEV standard for clinical visual evoked potentials: (2016 update). *Doc Ophthalmol*. 2016;133:1–9. doi:10.1007/s10633-016-9553-y.
12. Trick GL, Trick LR, Morris P, Wolf M. Visual field loss in senile dementia of the Alzheimer's type. *Neurology*. 1995;45:68–74. doi:10.1212/WNL.45.1.68.
13. Mendez MF, Mendez MA, Martin R, et al. Complex visual disturbances in Alzheimers disease. *Neurology*. 1990;40:439–443. doi:10.1212/WNL.40.3_Part_1.439.
14. Garcia-Martin ES, Rojas B, Ramirez AI, et al. Macular thickness as a potential biomarker of mild Alzheimer's disease. *Ophthalmology*. 2014;121:1149–1153. doi:10.1016/j.ophtha.2013.12.023.
15. Ascaso FJ, Cruz N, Modrego PJ, et al. Retinal alterations in mild cognitive impairment and Alzheimer's disease: an optical coherence tomography study. *J Neurol*. 2014;261:1522–1530. doi:10.1007/s00415-014-7374-z.
16. Cheung CY, Ong YT, Hilal S, et al. Retinal ganglion cell analysis using high-definition optical coherence tomography in patients with mild cognitive impairment and Alzheimer's Disease. J Alz Dis. 2015;45:45–56. doi:10.3233/JAD-141659.
17. Golzan SM, Goozee K, Georgevsky D, et al. Retinal vascular and structural changes are associated with amyloid burden in the elderly: ophthalmic biomarkers of preclinical Alzheimer's disease. *Alzheimers Res Ther*. 2017;1(9):13. doi:10.1186/s13195-017-0239-9.
18. Blanks JC, Schmidt SY, Torigoe Y, Porrello KV, Hinton DR, Blanks RH. Retinal pathology in Alzheimer's disease. II. Regional neuron loss and glial changes in GCL. *Neurobiol Aging*. 1996;17:385–395. doi:10.1016/0197-4580(96)00009-7.
19. Blanks JC, Torigoe Y, Hinton DR, Blanks RH. Retinal pathology in Alzheimer's disease. I. Ganglion cell loss in foveal/parafoveal retina. *Neurobiol Aging*. 1996;17:377–384. doi:10.1016/0197-4580(96)00010-3.
20. Williams PA, Thirgood RA, Oliphant H, et al. Retinal ganglion cell dendritic degeneration in a mouse model of Alzheimer's disease. *Neurobiol Aging*. 2013;34:1799–1806. doi:10.1016/j.neurobiolaging.2013.01.006.
21. Moschos MM, Markopoulos I, Chatziralli I, et al. Structural and functional impairment of the retina and optic nerve in Alzheimer's disease. Curr Alzh Res. 2012;9:782–788. doi:10.2174/156720512802455340.
22. Sartucci F, Borghetti D, Bocci T, et al. Dysfunction of the magnocellular stream in Alzheimer;s disease evaluated by pattern electroretinograms and visual evolved potentials. *Brain Res Bull*. 2010;82:169–176. doi:10.1016/j.brainresbull.2010.04.001.
23. Weinstein GW, Odom JV, Cavender S. Visually evoked potentials and electroretinography in neurologic evaluation. *Neurol Clin*. 1991;9:225–242. doi:10.1016/S0733-8619(18)30312-8.
24. Krasodomska K, Lubinski W, Potemkowski A, et al. Pattern electroretinogram (PERG) and pattern visual evoked potential (PVEP) in the early stages of Alzheimer's disease. *Doc Ophthalmol*. 2010;121:111–121. doi:10.1007/s10633-010-9238-x.
25. Kromer R, Serbecic N, Hausner L, Froelich L, Beutelspacher SC. Comparison of visual evoked potentials and retinal nerve fiber layer thickness in Alzheimer's disease. Front Neur. 2013;4:1–6. doi:10.3389/fneur.2013.00203.
26. Holder GE. Electrophysiological assessment of optic nerve disease. *Eye*. 2004;18:1133–1143. doi:10.1038/sj.eye.6701573.
27. Blanks JC, Hinton DR, Sadun AA, et al. Retinal ganglion cell degeneration in Alzheimer's disease. *Brain Res*. 1989;501:364–372. doi:10.1016/0006-8993(89)90653-7.
28. Koronyo-Hamaoui M, Koronyo Y, Ljubimov AV, et al. Identification of amyloid plaques in retinas from Alzheimer's patients and noninvasive in vivo optical imaging of retinal plaques in a mouse model. *Neuroimage*. 2011;54:S204–S217. doi:10.1016/j.neuroimage.2010.06.020.
29. Hoh KJ, Lenassi E, Jeffery G. Viewing ageing eyes: diversities of amyloid beta accumulation in the ageing mouse retina and the upregulation of macrophages. *PloS ONE*. 2010;5:e13127. doi:10.1371/journal.pone.0013127.
30. Perez SE, Lumayag S, Kovacs B, Mufson EJ, Xu S. Beta-amyloid deposition and functional impairment in the retina of the APPswe/PS1DeltaE9 transgenic mouse model of Alzheimer's disease. *Invest Ophthalmol Vis Sci*. 2009;50:793–800. doi:10.1167/iovs.08-2384.
31. Alexandrov PN, Pogue A, Bhattacharjee S, Lukiw WJ. Retinal amyloid peptides and complement factor H in transgenic models of Alzheimer's disease. *Neuroreport*. 2011;22:623–627. doi:10.1097/WNR.0b013e3283497334.
32. Dutescu RM, Li QX, Crowston J, et al. Amyloid precursor protein processing and retinal pathology in mouse models of Alzheimer's disease. *Graefe's Arch Clin Exp Ophthalmol*. 2009;247:1213–1221. doi:10.1007/s00417-009-1060-3.
33. Parthasarathy R, Chow KM, Derafshi Z, et al. Reduction of amyloid-beta levels in mouse eye tissues by intra-vitreally delivered neprilysin. *Exp Eye Res*. 2015;138:134–144. doi:10.1016/j.exer.2015.06.027.
34. Gupta VK, Chitranshi N, Gupta VB, et al. Amyloid beta accumulation and inner retinal degenerative changes in Alzheimer's disease transgenic mouse. *Neurosci Lett*. 2016;623:52–56. doi:10.1016/j.neulet.2016.04.059.
35. More SS, Vince R. Hyperspectral imaging signatures detect amyloidopathy in alzheimer's mouse retina well before onset of cognitive decline. *ACS Chem Neurosci*. 2015;6:306–315. doi:10.1021/cn500242z.
36. Maass A, Lockhart SN, Harrison TM, et al. Entorhinal tau pathology, episodic memory decline, and neurodegeneration in aging. *J Neurosci*. 2018;38:530–543. doi:10.1523/JNEUROSCI.2028-17.2017.
37. Schön C, Hoffmann NA, Ochs SM, et al. Long-term in vivo imaging of fibrillar tau in the retina of P301S transgenic mice. *PLoSONE*. 2012;7:e53547. doi:10.1371/journal.pone.0053547.
38. Pike KE, Savage G, Villemagne VL, et al. Beta amyloid imaging and memory in non-demented individuals: evidence for preclinical Alzheimer's disease. *Brain*. 2007;130:2837–2844. doi:10.1093/brain/awm238.
39. Fauw J, Ledsam JR, Romera-Paredes B, et al. Clinically applicable deep learning for diagnosis and referral in retinal disease. *Nat Med*. 2018;24:1342–1350. doi:10.1038/s41591-018-0107-6.
40. Wang T, Qiu RG, Yu M. Predictive modeling of the progression of Alzheimer's disease with recurrent neural networks. *Sci Rep*. 2018;8:9161. article number. doi:10.1038/s41598-018-27337-w.